THE JOURNAL OF BIOLOGICAL CHEMISTRY
Vol. 280, No. 27, Issue of July 8, pp. 25907–25912, 2005

Printed in U.S.A.

Double-spanning Plant Viral Movement Protein Integration into the Endoplasmic Reticulum Membrane Is Signal Recognition Particle-dependent, Translocon-mediated, and Concerted*

Received for publication, November 4, 2004, and in revised form, May 9, 2005
Published, JBC Papers in Press, May 11, 2005, DOI 10.1074/jbc.M412476200

Ana Saurí‡§, Suraj Saksena¶, Jesús Salgado‡, Arthur E. Johnson¶‖, and Ismael Mingarro‡ ‡‡**

*From the ‡Departament de Bioquímica i Biologia Molecular, Universitat de València E-46 100 Burjassot, Spain, the Departments of ¶Biochemistry and Biophysics and ‖Chemistry, Texas A&M University, College Station, Texas 77843, and the **Department of Medical Biochemistry and Genetics, Texas A&M University System Health Science Center, College Station, Texas 77843-1114*

The current model for cell-to-cell movement of plant viruses holds that transport requires virus-encoded movement proteins that intimately associate with endoplasmic reticulum membranes. We have examined the early stages of the integration into endoplasmic reticulum membranes of a double-spanning viral movement protein using photocross-linking. We have discovered that this process is cotranslational and proceeds in a signal recognition particle-dependent manner. In addition, nascent chain photocross-linking to Sec61α and translocating chain-associated membrane protein reveal that viral membrane protein insertion takes place via the translocon, as with most eukaryotic membrane proteins, but that the two transmembrane segments of the viral protein leave the translocon and enter the lipid bilayer together.

A particularly important requirement for plant virus infection at an early stage involves the ability of a virus to move from cell to cell. Transport of viruses between plant cells requires the function of virus-encoded movement proteins. These proteins participate actively in the intra- and intercellular transport of viral genomes to such an extent that movement protein dysfunction hinders viral infection (1). Plant viruses have evolved different strategies for cell-to-cell movement. One of these strategies involves the passage of complexes of the viral genome and movement proteins through the plasmodesmata, the membranous channels formed by prolongations of the ER[1] membranes that interconnect cells in higher plants. It is now clear that several of these virus-encoded proteins associate with ER membranes (2–4), although the path by which they reach the membrane has not yet been explored. Clearly, the success of viral infection relies on the correct targeting and integration of the viral movement proteins into the ER membrane. In this report, we focus on the biogenesis of one of these movement proteins that associates with ER membranes to unravel the mechanism used by these proteins to reach and integrate into the biological membranes.

Two alternative pathways for targeting membrane proteins to the ER membrane are recognized: a cotranslational or signal recognition particle (SRP)-dependent pathway and a post-translational or SRP-independent pathway (5). However, the majority of integral membrane proteins are targeted through the SRP pathway to the membrane of the ER in eukaryotic cells or to the bacterial inner membrane in prokaryotic cells. SRP targets the nascent membrane protein-ribosome-mRNA complex to the membrane by interacting with the membrane-bound SRP receptor. The SRP receptor is presumably located adjacent to a protein-conducting channel, the so-called translocon (5), that is comprised in eukaryotic cells of the Sec61 α, β, and γ subunits (6) and the translocating chain-associated membrane protein (TRAM) (7). After targeting, the translocon facilitates the integration and lateral exit of nascent membrane protein TM segments into the ER membrane (5, 8, 9). The translocon has been described in all kingdoms of life, and the bacterial SecYEG complex is homologous to the Sec61 complex (10), whereas YidC may be a functional homologue of TRAM (11).

Despite the identification of key components that target and insert cellular membrane proteins, the mechanism of insertion of viral membrane proteins into the host membrane is poorly understood. The current knowledge is mainly based in studies focused on small bacteriophage-coat proteins, such as M13 procoat and Pf3. These proteins have long been considered to insert into the host cell membrane by a spontaneous mechanism (12, 13), although recently it has been demonstrated that in both cases, YidC mediates the membrane insertion of these SRP/translocon-independent bacteriophage proteins (reviewed in Ref. 14). As for viral protein integration in eukaryotic cells, intensive studies have been carried out with animal viral proteins (reviewed in Ref. 15) or insect-derived viral proteins (9). Nevertheless, it has to be mentioned that the above-mentioned viral proteins are all single spanning membrane proteins and that there is no information regarding plant viral membrane protein integration to date.

To investigate the membrane targeting and insertion of plant viral membrane proteins into the ER membrane and the mechanism by which a polytopic viral membrane protein integrates into the lipid bilayer, we have examined p9, a double-spanning viral movement protein from carnation mottle carmovirus. The genome of this virus is a single-stranded RNA encoding five proteins, two of them being the small movement

* This work was supported by Grants BMC2003-01532 from the Spanish MCyT and GV04B-183 from the Generalitat Valenciana (to I. M.) and by National Institutes of Health Grant R01 GM26494 and by the Robert A. Welch Foundation (to A. E. J.). The costs of publication of this article were defrayed in part by the payment of page charges. This article must therefore be hereby marked "*advertisement*" in accordance with 18 U.S.C. Section 1734 solely to indicate this fact.

§ A recipient of a predoctoral fellowship from the Spanish Ministerio de Educación y Ciencia.

‡‡ To whom correspondence should be addressed. Tel.: 34-96-354-3796; Fax: 34-96-354-4635; E-mail: Ismael.Mingarro@uv.es.

[1] The abbreviations used are: ER, endoplasmic reticulum; CRM, column-washed rough ER microsomes; EKRM, salt-washed ER membranes; IP, immunoprecipitation; Lep, leader peptidase; RNC, ribosome-nascent chain complex; SRP, signal recognition particle; TM, transmembrane; TRAM, translocating chain-associating membrane protein; ϵANB-Lys-tRNA^{amb}, Nϵ-(5-azido-2-nitrobenzoyl)-Lys-tRNA^{amb}.

proteins, p9 and p7. The latter has been shown to have RNA binding capacity (16), whereas the interaction of the RNA-p7 complex with the membrane-anchored p9 protein would facilitate the cell-to-cell viral transport through the membranous plasmodesmata channels (2). It is thus important to gain knowledge concerning the mechanism by which this non-cellular p9 protein is targeted and inserted into the ER membrane to dissect the infection process of these plant viruses.

For this purpose, we used a site-directed photocross-linking approach to demonstrate that p9 is inserted cotranslationally into the ER membrane by the cell machinery in an SRP- and translocon-mediated fashion. In addition, photocross-linking to TRAM was observed for both TM segments of p9, although many membrane protein TM segments do not photocross-link to TRAM (17–20). Thus, plant viral membrane protein integration appears to utilize the translocon apparatus and associated factors of the host to achieve targeting to and integration into the ER membrane, although the viral and host processes may differ somewhat with respect to the interaction with associated components such as TRAM. In addition, we observed that both TM sequences of the viral protein remain in the translocon until the termination of translation, suggesting that partition of the protein into the lipid bilayer occurs in a concerted manner.

MATERIALS AND METHODS

Plasmids and tRNA—For *in vitro* translation, the p9 sequence (without a stop codon) was inserted after the SP6 promoter, and the C terminus of p9 was fused to the P2 domain of the *Escherichia coli* leader peptidase sequence in a pGEM-1 plasmid as in Ref. 2 (p9-P2). For photocross-linking experiments, threonine at position 15 and serine at position 49 were converted to amber codons (TAG) by site-directed mutagenesis using the QuikChange mutagenesis kit from Stratagene (La Jolla, CA) according to the manufacturer's instructions. Oligonucleotides purchased were from Isogen (Maarssen, The Netherlands) and Integrated DNA Technologies (Coralville, IA). Nϵ-(5-azido-2-nitrobenzoyl)-Lys-tRNA^{amb} (ϵANB-Lys-tRNA^{amb}) was prepared as before (8, 21).

Cotranslational and Post-translational Insertion Assays—Full-length p9 DNA was amplified from the p9-P2 plasmid by PCR using a reverse primer with a stop codon at the end of the p9 sequence. PCR products were transcribed *in vitro* using purified SP6 RNA polymerase (37 °C, 2 h) as before (8, 9). *In vitro* translations (typically 25 μl, 26 °C, 40 min) were performed using wheat germ cell-free extract as before (8, 9, 22) in the presence of 40 nM purified SRP, 4 eq of canine column-washed rough ER microsomes (CRMs) or canine salt-washed ER membranes (EKRMs) (23), and 5 μCi of [^{35}S]Met. For post-translational incubations with membranes, translation incubations were inhibited with cycloheximide (2 mg/ml final) for 10 min at 26 °C before CRMs were added and incubated for an additional 30 min. Microsomes were recovered by centrifugation through a sucrose cushion (4 °C, 4 min, 100,000 $\times$ *g*) and resuspended in sample buffer before SDS-PAGE analysis. Radioactive photoadducts were detected using a Bio-Rad FX phosphorimaging device.

Photocross-linking Experiments—Truncated mRNAs were generated by PCR using different reverse primers that lacked a stop codon to obtain nascent chains of a specific length. PCR products were *in vitro* transcribed using purified SP6 RNA polymerase as above. For SRP photocross-linking experiments, *in vitro* translation (typically 50 μl, 26 °C, 40 min) of a 70-residue nascent chain was performed as before (9, 24) in a wheat germ cell-free extract containing 40 nM SRP, 100 μCi of [^{35}S]Met, and 32 pmol of ϵANB-Lys-tRNA^{amb}. After translation, samples were incubated 12 min on ice prior to a 15-min irradiation on ice using a 500 watt mercury arc lamp. Photolyzed samples were sedimented through a 120-μl sucrose cushion (0.5 M sucrose, 20 mM HEPES (pH 7.5), 4 mM $Mg(OAc)_2$, 100 mM KOAc) using a TLA100 rotor (Beckman Instruments; 100,000 rpm; 4 min; 4 °C) to recover the RNC·SRP complexes. Pellets were resuspended in sample buffer before analysis by SDS-PAGE and detection by phosphorimaging as before (8, 9).

To assess Sec61α and TRAM photocross-linking, truncated mRNAs were translated as described above except that samples contained 8 eq of CRMs. Samples were photolyzed and sedimented as above prior to sample immunoprecipitation.

Immunoprecipitation—For Sec61α, pelleted membranes were resuspended in 50 μl of 0.25% (w/v) SDS, 100 mM Tris-HCl (pH 7.5) and incubated at 55 °C for 30 min. In the case of TRAM, pelleted membranes were resuspended in 50 μl of 1% (w/v) SDS, 100 mM Tris-HCl (pH 7.6) and incubated at 55 °C for 30 min. Samples were washed three times with 150 μl of buffer A (140 mM NaCl, 10 mM Tris-HCl (pH 7.5), 2% (v/v) Triton X-100) for Sec61α immunoprecipitation (IP) and with buffer B (150 mM NaCl, 50 mM Tris-HCl (pH 7.5), 2% (v/v) Triton X-100, 0.2% (w/v) SDS) for TRAM IP. Samples were precleared by rocking with 40 μl of buffer A/B-washed protein A-Sepharose (Sigma) at room temperature for 1 h. After removal of the beads by centrifugation at room temperature, supernatants were incubated with affinity-purified rabbit antisera specific for Sec61α or TRAM (Research Genetics, Huntsville, AL) overnight at 4 °C. Then 40 μl of protein A-Sepharose, previously equilibrated with buffer A or B, were added and incubated for 4 h at 4 °C. After sedimentation, the beads were washed twice with 750 μl of buffer A or B followed by a final washing in the same buffer without detergent. Samples were prepared for SDS-PAGE analysis by the addition of sample buffer and incubation at 37 °C for 10 min. Results were visualized and processed using the Bio-Rad FX phosphorimaging device.

RESULTS AND DISCUSSION

Cotranslational and SRP-dependent Insertion of p9—Integration of p9 into ER-derived microsomes can be monitored by glycosylation. This modification is performed by the oligosaccharyl transferase enzyme, which is adjacent to the translocon. Oligosaccharyl transferase adds sugar residues cotranslationally to a N*X*(S/T) consensus sequence (25), with *X* being any amino acid except proline (26), after the protein emerges from the translocon pore. Glycosylation of a protein translated *in vitro* in the presence of microsomal membranes therefore indicates the exposure of the nascent chain to the oligosaccharyl transferase active site on the lumenal side of the ER membrane (27).

Using a glycosylation mapping strategy, the topology of integrated p9, which has both its N and C terminus facing the cytoplasmic side of the membrane, was established previously (2). This topology was demonstrated using a mutant variant of p9 (Fig. 1*A*), termed here p9$_{EEE}$, in which insertion of the second TM segment (TM2) was precluded by the introduction of three glutamic acids in the middle of this TM hydrophobic region. Additionally, a glycosylation sequon was engineered at the C-terminal domain of p9$_{EEE}$.

When full-length p9$_{EEE}$ was translated *in vitro* in the presence of CRMs containing SRP, much of the protein was glycosylated (Fig. 1*B*, *lane 1*), as shown by the increase in electrophoretic mobility of the slower radioactive p9$_{EEE}$ band after an endoglycosidase H treatment (Fig. 1*B*, *lane 2*). However, when the CRMs were added post-translationally, after inhibition of protein synthesis with cycloheximide, no p9$_{EEE}$ was glycosylated in the absence or presence of SRP (Fig. 1*B*, *lanes 3* and *4*). Furthermore, these unglycosylated forms of p9$_{EEE}$ did not integrate into the membrane, as they were soluble upon alkaline extraction (data not shown), thereby demonstrating that p9$_{EEE}$ cannot target and integrate post-translationally. The SRP dependence of p9$_{EEE}$ targeting (Fig. 1*B*) was further demonstrated by using microsomes that had been stripped of their SRP and residual ribosomes by washing in EDTA and high salt (EKRMs) (23). p9$_{EEE}$ proteins were only glycosylated when EKRMs were added at the beginning of the translation along with purified SRP (Fig. 1*B*, *lane 6*). Thus, targeting, translocation, integration, and glycosylation of p9$_{EEE}$ are all SRP-dependent events that occur cotranslationally.

The above results suggest that p9 contains a signal sequence that directs the ribosome-nascent chain complex (RNC) synthesizing this protein to the translocon via an SRP-dependent pathway. If this were true, one would predict that the first TM segment of p9 (TM1) would constitute a signal sequence and bind to SRP54, the 54-kDa subunit of SRP (24, 28). A direct method for detecting this type of interaction consists of positioning a photoreactive probe in the signal sequence, where it would be expected to photocross-link to SRP54 upon illumination with UV light (24, 28). Radiolabeled, fully assembled

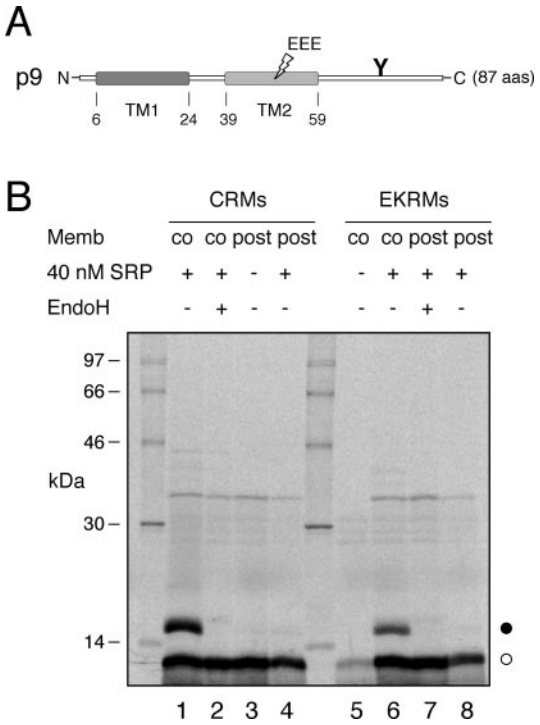

FIG. 1. **Targeting of p9 to the ER membrane (*Memb*) is cotranslational and SRP-dependent.** *A*, structural organization of p9. A glycosylation site was introduced into p9 at codon 72 for topology studies (2), as were 3 Glu residues in the middle of the second TM fragment of $p9_{EEE}$. *B*, radiolabeled full-length $p9_{EEE}$ protein translation was performed in the presence of either CRMs (*left*) or EKRMs (*right*) and in the presence (+) or absence (−) of SRP as indicated. In some cases, samples were treated with endoglycosidase H (*EndoH*) prior to SDS-PAGE. Microsomes were added during p9 translation (*co*) or after inhibition of translation with 2 mg/ml of cycloheximide (*post*). The *solid circle* identifies the glycosylated $p9_{EEE}$, whereas the *open circle* indicates the non-glycosylated $p9_{EEE}$ polypeptides.

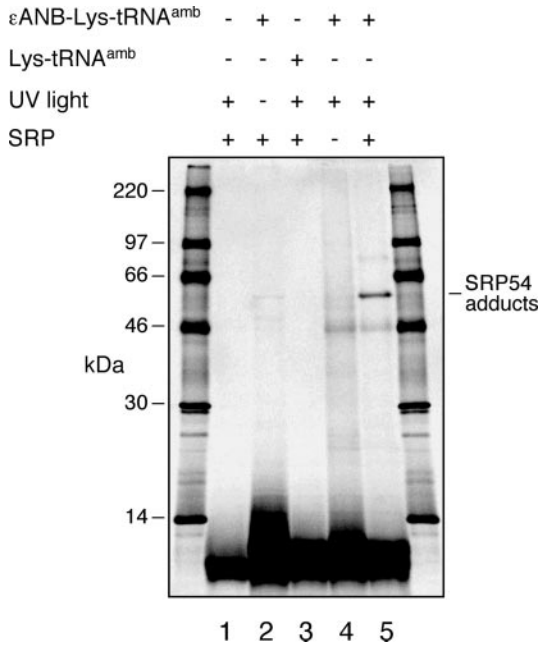

FIG. 2. **Photocross-linking of p9 to SRP.** A single photoreactive probe was incorporated by positioning an amber stop codon at position 15. RNCs containing 70-residue radioactive nascent chains were prepared in the presence of unmodified Lys-tRNA^{amb} or photoreactive ϵANB-Lys-tRNA^{amb} as indicated. Only the sample in *lane 2* was not exposed to UV light, and only the sample in *lane 4* lacked SRP.

translation intermediates can be prepared *in vitro* by translating, in the presence of [^{35}S]Met, mRNAs that are truncated within the coding region. A ribosome halts when it reaches the end of such an mRNA, but the nascent chain does not dissociate from the tRNA-ribosome complex because the absence of a stop codon prevents normal termination from occurring. A photoreactive probe can then be selectively incorporated into the nascent polypeptide by including in the translation reaction a modified amber suppressor aminoacyl-tRNA (ϵANB-Lys-tRNA^{amb}) that recognizes and translates an amber stop codon positioned in the truncated mRNA sequence (8, 9).

To use the above strategy, an amber stop codon was substituted roughly in the middle of TM1, at codon 15 of p9, to yield p9St15. A truncated mRNA encoding 70 residues of p9St15 was transcribed from this DNA and translated in the presence or absence of SRP and either ϵANB-Lys-tRNA^{amb} or unmodified Lys-tRNA^{amb} (Fig. 2). In each case, the incubation lacked microsomes and thus generated only the RNC·SRP intermediate. The 70-residue nascent chain was chosen to ensure that TM1 was outside the ribosome exit tunnel and accessible for binding to SRP. Upon illumination, a ~61-kDa photoadduct was formed only in the presence of added SRP (Fig. 2, *lane 5*). As expected, no photoadduct was observed in the absence of SRP (Fig. 2, *lane 4*), UV light (Fig. 2, *lane 2*), or a photoreactive probe (Fig. 2, *lanes 1* and *3*). The apparent molecular mass of the photoadduct corresponds to an adduct between the 70-residue nascent chain and SRP54 (9, 24), thereby suggesting that the TM1 segment of p9 acts as a signal sequence and associates with the SRP54 subunit of SRP to form a complex that targets the RNC to the translocon.

These results demonstrated that plant viral p9 movement protein biogenesis is cotranslational and that p9 reaches the ER membrane in an SRP-dependent manner, which clearly differs from bacterial virus coat proteins that insert into the membrane in an SRP-independent manner. It seems likely that the SRP dependence of p9 plant viral protein targeting to the ER membrane ensures that the viral protein is integrated into a specific membrane, the ER membrane, that initiates and facilitates the proper sorting and transport of the viral genome to adjacent cells through the plasmodesmata membrane system.

p9 Is Integrated through the Translocon—After demonstrating that p9 is targeted to the ER membrane through an SRP-dependent process, we focused on determining whether this viral membrane protein is adjacent to translocon proteins after targeting, as has been observed in a number of previous photocross-linking studies with eukaryotic or model membrane proteins (reviewed in Refs. 5 and 29). To identify proteins adjacent to p9 nascent chains during membrane insertion, integration intermediates containing nascent p9 chains of increasing length (Fig. 3) were prepared using CRMs and then photolyzed. Photoactivatable probes were incorporated by the translation of truncated mRNAs with amber codons at position 15 (p9St15, Fig. 3*B*) or 49 (p9St49, Fig. 3*C*) in the presence of ϵANB-Lys-tRNA^{amb}. The probes were therefore located roughly in the middle of the p9 TM segments (Fig. 3*A*). Since native p9 is a small protein with only 87 amino acids, it was necessary to elongate its C-terminal domain to examine RNCs with long nascent chains and thereby trap the p9 in the RNC-translocon complex by preventing the termination of protein synthesis and the release of p9 from the translocon. To accomplish this, we used the extramembranous P2 domain of the *E. coli* leader peptidase (Lep) (see "Materials and Methods" for cloning details) and generated p9 truncates of different lengths by PCR, using 3′ primers that anneal at selected positions.

After photolysis, the extent of photocross-linking of each p9 derivative to Sec61α was determined by IP using affinity-purified antibodies to Sec61α. As shown in Fig. 3*B*, the probe in

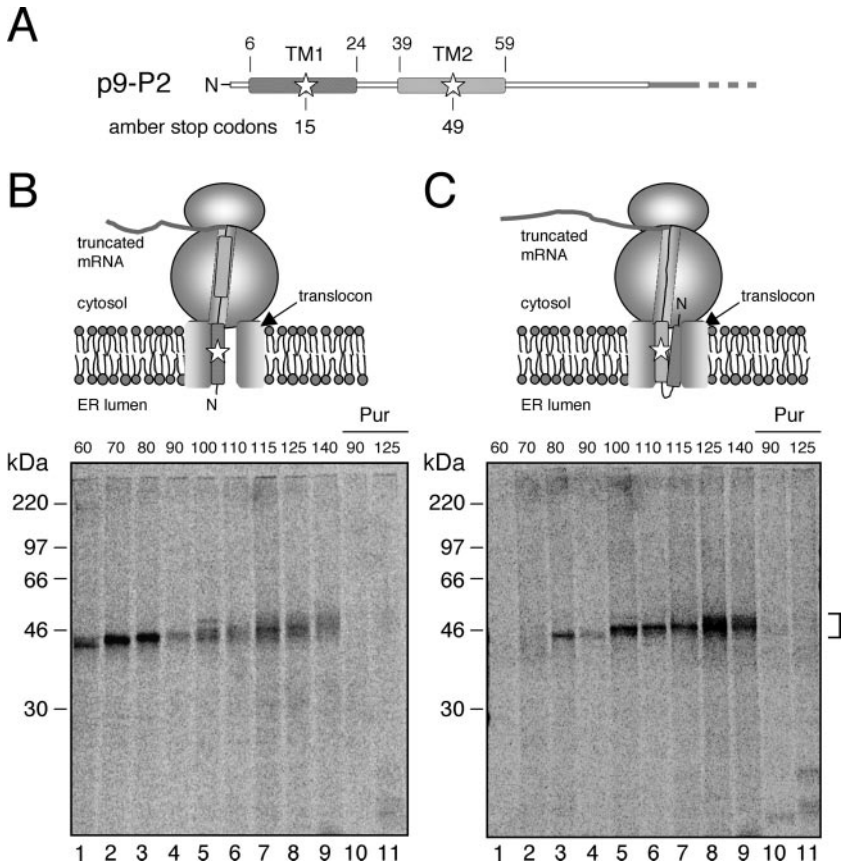

FIG. 3. **Photocross-linking of p9 nascent chains to Sec61α.** *A*, structural organization of the p9 protein. *B* and *C*, p9 RNCs with radioactive nascent chains of different lengths (60–140 residues, numbered at the top of the gels) and carrying a single photoreactive probe either at position 15 in TM1 (*B*) or at position 49 in TM2 (*C*) were targeted to CRMs and then photolyzed. Photoadducts containing Sec61α were purified by IP and analyzed by SDS-PAGE. The *star* signals the amber stop codon sites in *panel A* and the photoactivatible amino acid position in *panels B* and *C*. The *bracket* signals the IP photoadducts increased in size as the nascent chain lengthened. In *lanes 10* and *11*, 2 mM puromycin (*Pur*) was added (26 °C, 30 min) to release nascent chains from the ribosome prior to photolysis.

TM1 (p9St15) reacts covalently with Sec61α at all nascent chain lengths tested, with intermediates of 70 and 80 amino acids showing the highest extents of photocross-linking. As expected, the p9-Sec61α photoadducts increased in size as the nascent chain lengthened, as shown by the gradual increase in apparent molecular mass of the photoadduct (Fig. 3*B*). These data also reveal that some TM1 segments remain adjacent to Sec61α in the translocon long after TM2 reaches the pore, and these TM segments apparently partition into the bilayer only after being released from the ribosome.

In contrast, when the probe is located at position 49 (p9St49) in TM2, a nascent chain at least 80 residues long is required to observe photoadducts with translocon proteins (Fig. 3*C*). This delayed cross-linking nicely matches the delayed incorporation of the probe into p9 and is consistent with the requirement of about 30 residues between the amber stop codon and the ribosomal peptidyl transferase site (P-site) before the probe exits the ribosomal tunnel and is exposed to translocon proteins. As with the TM1 probe, TM2 remained adjacent to Sec61α until termination (Fig. 3*C*). When nascent chains were released from the ribosome by puromycin, neither p9St15 nor p9St49 was cross-linked to Sec61α(Fig. 3, *B* and *C*, *lanes 10* and *11*). Thus, both TM1 and TM2 diffused away from the translocon and into the membrane only after release of the p9 nascent chain from the tRNA in the P-site prior to photolysis.

Are TM1 and TM2 Insertion Coupled?—The molecular details of the integration of multispanning membrane proteins are largely unknown. p9, a double-spanning membrane protein, falls into the simplest category of such proteins and thus provides some clues about this process. Two of the several possible mechanisms for the integration of membrane proteins containing two TM sequences are: (i) a "linear insertion model" (30), in which membrane integration of TM1 occurs independently of the appearance at the translocon of TM2; or (ii) a "concerted model," in which both TM segments of the nascent protein bind to one or more translocon proteins and are held until the termination of translation, being then released laterally as a group (a helical hairpin for double-spanning proteins) into the lipid phase (8).

After preparing integration intermediates with nascent chains of different lengths, we observed that both TM segments from p9 were in proximity to Sec61α, even when the nascent chain was long enough for the TM segments to exit the translocon individually (Fig. 3), thereby indicating that they integrate together into the lipid bilayer as a helical hairpin. Furthermore, the extent of photoadduct formation with TM2 did not decrease significantly as the length of the nascent chain increased, although the length of the nascent chain tether to the ribosome was enough for TM2 (and TM1) diffusion away from the translocon. For example, the distance between the end of TM2 (residue 59, Fig. 3*A*) and the tRNA in the ribosomal P-site is about 81 residues for a 140-residue nascent chain. Even if 35 residues are located in the ribosomal tunnel, the nascent chain tether from the ribosomal exit site to the C-terminal end of TM2 would span ~45 residues, or more than 150 Å of a fully extended polypeptide, a length clearly sufficient to allow TM2 to move away from Sec61α. Thus, from these data, it appeared that p9 follows a bundling insertion mechanism because both TM segments remain in the translocon until the termination of translation and integrate into the lipid bilayer together. The most likely explanation for the long retention of the TM segments in the translocon is that protein-protein interactions between the TM segments and the translocon proteins mediate TM segment release into the bilayer, as has been observed previously (8, 9).

These results differed markedly from the previously reported behavior of double-spanning membrane proteins derived from Lep. In the latter case, RNCs with nascent chains of 95 residues (or longer) and a photoreactive probe in the middle of the first TM fragment cross-link very weakly with Sec61α, and

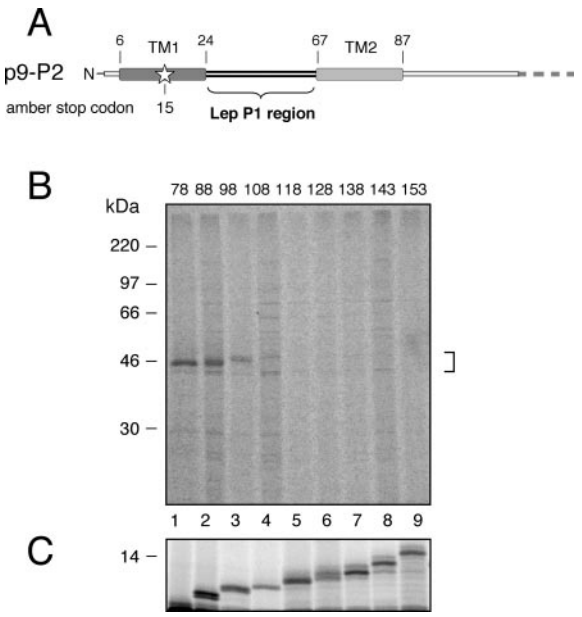

FIG. 4. **Photocross-linking to Sec61α of nascent chains of a p9 chimera containing the loop (P1 region) of Lep.** *A*, structural organization of the chimeric protein, stressing in *bold* the Lep region. The *star* signals the amber stop codon site. *B*, nascent p9 chimeric proteins of different lengths (78–153 residues) were translated in the presence of microsomes and photolyzed as described in the legend for Fig. 3. Photoadducts containing Sec61α were purified by IP and analyzed by SDS-PAGE. *C*, before the sample was subjected to IP with Sec61α antisera, equal aliquots of each sample were removed and directly analyzed by SDS/PAGE to detect and quantify the total radioactive translation products. The *bracket* signals the IP photoadducts.

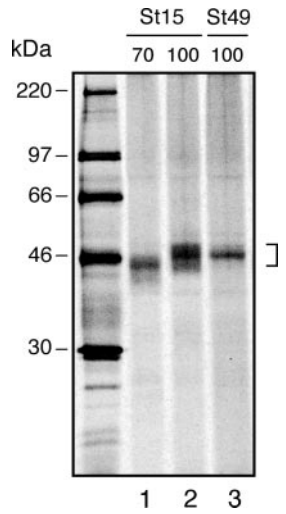

FIG. 5. **Photocross-linking of p9 nascent chains to TRAM.** Integration intermediates containing radioactive nascent chains of 70 or 100 residues were photolyzed and examined by IP as described in the legend for Fig. 3 but using antibodies specific for TRAM. The photoreactive probe was located in TM1 at position 15 (*St15*) for the samples in *lanes 1* and *2*, whereas the probe was located in TM2 at position 49 (*St49*) for the sample in *lane 3*. The *bracket* signals the photoadducts.

both TM segments leave the eukaryotic translocation channel long before the termination of translation (17). Moreover, a linear integration of the two TM fragments of Lep has also been proposed in a recent study using *E. coli* inner membrane vesicles (31). To what extent are the apparent differences between the Lep results and those reported here explained by the difference in the lengths of the loops separating the TM segments in the two proteins? To address this question, we prepared a chimera in which the 42 residues of P1, the extramembranous region that connects the two TM segments in Lep, replaced the 14 residues that constitute the loop between the two TM segments of p9 (Fig. 4*A*). Nascent chains of different lengths were then synthesized in the presence of CRMs. An aliquot of each sample was irradiated with UV light, whereas the remainder indicated the extent of nascent chain production (Fig. 4*C*). Irradiated samples were subjected to IP using affinity-purified antibodies to Sec61α(Fig. 4*B*).

With RNCs containing nascent chains that were 78 and 88 amino acids in length, strong cross-links to Sec61α were detected (Fig. 4*B*, *lanes 1* and *2*). At these chain lengths, the RNC complex was targeted to the membrane, where the first TM segment contacts Sec61α. For all chain lengths longer than 98 residues, little or no photocross-linking to Sec61α was observed, indicating that TM1 of p9 has partitioned into the lipid bilayer, a result that clearly differs from what was observed with wild type p9 (compare Fig. 4*B* with Fig. 3*B*). Thus, although the larger loop in the modified p9 protein allowed lateral diffusion of its first TM segment away from the translocon, the shorter loop in natural p9 RNCs prevents the independent diffusion of the two TM segments into the bilayer. It therefore seems likely that integration of p9 into the ER membrane in a functional state, and perhaps proper sorting of p9 *in vivo*, requires the concerted insertion of TM1 and TM2 into the bilayer. Since TM2 is slightly less hydrophobic than TM1 (-3.67 kcal/mol *versus* -4.41 kcal/mol, as calculated from the White-Wimley values ($\Delta G_{woct} - \Delta G_{wif}$) (32)), then possibly TM1 must leave the translocon with TM2 to ensure that TM2 is inserted efficiently into the ER membrane. Interestingly, a similar bundling insertion model has been observed for mannitol permease, a polytopic membrane protein with a short interconnecting loop between the first two TM segments (33).

TRAM Protein Is Adjacent to p9 during Integration—Another protein component of the translocon, TRAM, has been photocross-linked to several different nascent secretory and membrane proteins (5). However, the extent of TRAM cross-linking varies tremendously for different membrane proteins (8, 9, 17–19, 22, 34). To assess the proximity of p9 TM1 and TM2 to TRAM and its possible involvement in p9 integration, we examined the extent of p9 photocross-linking to TRAM by immunoprecipitation with affinity-purified antibodies specific for TRAM. As shown in Fig. 5, probes in TM1 and TM2 both reacted covalently with TRAM after photolysis. Cross-linking was observed for nascent chains as short as 70 residues, indicating that TRAM is proximal to TM1 even at an early stage of p9 integration. Consistently, simultaneous cross-linking of both TM fragments (100-residue-long RNCs; Fig. 5, *lanes 2* and *3*) with TRAM suggests that TM1 and TM2 partition into the lipid bilayer as a helical hairpin. It is also worth noting that the extent of TM1-TRAM photocross-linking increases as the nascent chain length increases from 70 to 100 residues (Fig. 5, compare *lanes 1* and *2*), whereas the extent of TM1-Sec61α photocross-linking decreases as the nascent chain lengthens from 70 to 100 residues (Fig. 3*B*, compare *lanes 2* and *5*). Thus, although TM1 and TM2 are adjacent to both Sec61α and TRAM throughout p9 integration, the positioning of TM1 and TM2 within the translocon may vary at different stages of integration.

Although several TM segments are apparently never adjacent to TRAM (8), the vesicular stomatitis virus G TM α-helix (8, 22) and the TM segments of two viral envelope membrane proteins of the baculovirus occlusion-derived virus (9) are positioned near TRAM in the translocon. Since p9 is also a viral membrane protein, it is conceivable that TRAM has a specific role in the mechanism of membrane integration of these "foreign" proteins, perhaps by usurping a natural host selectivity function of TRAM during integration (9).

Conclusion—Plant virus movement proteins may generally

interact with cellular macromolecules through hydrophobic interactions (35). Several of these proteins are known to be associated with membranes (2–4). The results presented in this study indicated that the carmovirus movement protein, p9, is targeted to the ER membrane in a cotranslational/SRP-dependent fashion, in which membrane insertion proceeds through the translocon, as for most host membrane proteins. The simultaneous Sec61α and TRAM cross-linking to both TM segments suggested that the translocon assists in the assembly of this viral membrane protein before *en bloc* release into the lipid bilayer. Thus, partitioning of wild type p9 into the bilayer only occurs after the nascent membrane protein is released from the ribosome. The concerted insertion of TM1 and TM2 into the bilayer is ensured by the short loop connecting the two TM segments of p9. Whether the viral TM sequences interact with Sec61α and TRAM in the same manner as host TM sequences has yet to be determined. Dissection of these processes will shed light in our understanding of the role of the cellular endomembrane system in sorting and delivering viral movement proteins to the plasmodesmata as a part of the mechanism of viral infection.

Acknowledgments—We thank Yuanlong Shao, Yiwei Miao, and Cristina Moya for excellent technical assistance.

REFERENCES

1. McLean, B. G., Waigmann, E., Citovsky, V., and Zambryski, P. (1993) *Trends Microbiol.* **1,** 105–109
2. Vilar, M., Sauri, A., Monne, M., Marcos, J. F., von Heijne, G., Perez-Paya, E., and Mingarro, I. (2002) *J. Biol. Chem.* **277,** 23447–23452
3. Mitra, R., Krishnamurthy, K., Blancaflor, E., Payton, M., Nelson, R. S., and Verchot-Lubicz, J. (2003) *Virology* **312,** 35–48
4. Peremyslov, V. V., Pan, Y. W., and Dolja, V. V. (2004) *J. Virol.* **78,** 3704–3709
5. Johnson, A. E., and van Waes, M. A. (1999) *Annu. Rev. Cell Dev. Biol.* **15,** 799–842
6. Görlich, D., and Rapoport, T. A. (1993) *Cell* **75,** 615–630
7. Görlich, D., Hartmann, E., Prehn, S., and Rapoport, T. A. (1992) *Nature* **357,** 47–52
8. McCormick, P. J., Miao, Y., Shao, Y., Lin, J., and Johnson, A. E. (2003) *Mol. Cell* **12,** 329–341
9. Saksena, S., Shao, Y., Braunagel, S. C., Summers, M. D., and Johnson, A. E. (2004) *Proc. Natl. Acad. Sci. U. S. A.* **101,** 12537–12542
10. Schnell, D. J., and Hebert, D. N. (2003) *Cell* **112,** 491–505
11. Chen, M., Xie, K., Jiang, F., Yi, L., and Dalbey, R. E. (2002) *Biol. Chem.* **383,** 1565–1572
12. Geller, B. L., and Wickner, W. (1985) *J. Biol. Chem.* **260,** 13281–13285
13. Rohrer, J., and Kuhn, A. (1990) *Science* **250,** 1418–1421
14. de Gier, J. W., and Luirink, J. (2003) *EMBO Rep.* **4,** 939–943
15. Smith, A. E., and Helenius, A. (2004) *Science* **304,** 237–242
16. Vilar, M., Esteve, V., Pallas, V., Marcos, J. F., and Perez-Paya, E. (2001) *J. Biol. Chem.* **276,** 18122–18129
17. Heinrich, S. U., and Rapoport, T. A. (2003) *EMBO J.* **22,** 3654–3663
18. Mothes, W., Heinrich, S., Graf, R., Nilsson, I., von Heijne, G., Brunner, J., and Rapoport, T. (1997) *Cell* **89,** 523–533
19. Meacock, S. L., Lecomte, F. J., Crawshaw, S. G., and High, S. (2002) *Mol. Biol. Cell* **13,** 4114–4129
20. Laird, V., and High, S. (1997) *J. Biol. Chem.* **272,** 1983–1989
21. Flanagan, J. J., Chen, J. C., Miao, Y., Shao, Y., Lin, J., Bock, P. E., and Johnson, A. E. (2003) *J. Biol. Chem.* **278,** 18628–18637
22. Do, H., Falcone, D., Lin, J., Andrews, D. W., and Johnson, A. E. (1996) *Cell* **85,** 369–378
23. Walter, P., and Blobel, G. (1983) *Methods Enzymol.* **96,** 84–93
24. Krieg, U. C., Walter, P., and Johnson, A. E. (1986) *Proc. Natl. Acad. Sci. U. S. A.* **83,** 8604–8608
25. Silberstein, S., and Gilmore, R. (1996) *FASEB J.* **10,** 849–858
26. Shakin-Eshleman, S. H., Spitalnik, S. L., and Kasturi, L. (1996) *J. Biol. Chem.* **271,** 6363–6366
27. Nilsson, I., Kelleher, D. J., Miao, Y., Shao, Y., Kreibich, G., Gilmore, R., von Heijne, G., and Johnson, A. E. (2003) *J. Cell Biol.* **161,** 715–725
28. Kurzchalia, T. V., Wiedmann, M., Girshovich, A. S., Bochkareva, E. S., Bielka, H., and Rapoport, T. A. (1986) *Nature* **320,** 634–636
29. Alder, N. N., and Johnson, A. E. (2004) *J. Biol. Chem.* **279,** 22787–22790
30. Blobel, G. (1980) *Proc. Natl. Acad. Sci. U. S. A.* **77,** 1496–1500
31. Houben, E. N., Ten Hagen-Jongman, C. M., Brunner, J., Oudega, B., and Luirink, J. (2004) *EMBO Rep.* **5,** 970–975
32. White, S. H., and Wimley, W. C. (1999) *Annu. Rev. Biophys. Biomol. Struct.* **28,** 319–365
33. Beck, K., Eisner, G., Trescher, D., Dalbey, R. E., Brunner, J., and Muller, M. (2001) *EMBO Rep.* **2,** 709–714
34. Heinrich, S. U., Mothes, W., Brunner, J., and Rapoport, T. A. (2000) *Cell* **102,** 233–244
35. Mushegian, A. R., and Koonin, E. V. (1993) *Arch. Virol.* **133,** 239–257